

# Enhancing RNA Repair Efficiency by Combining Trans-splicing Ribozymes That Recognize Different Accessible Sites on a Target RNA

Ning Lan,<sup>\*</sup> Barbara L. Rooney,<sup>†</sup> Seong-Wook Lee,<sup>\*,1</sup> Richard P. Howrey,<sup>‡</sup> Clayton A. Smith,<sup>†</sup> and Bruce A. Sullenger,<sup>\*,2</sup>

<sup>\*</sup>Center for Genetic and Cellular Therapies, Department of Surgery and Department of Genetics, Duke University Medical Center, Durham, North Carolina 27710

<sup>‡</sup>Center for Genetic and Cellular Therapies, Department of Pediatrics, Duke University Medical Center, Durham, North Carolina 27710

<sup>†</sup>Center for Genetic and Cellular Therapies, Department of Medicine, Duke University Medical Center, Durham, North Carolina 27710

Received for publication May 24, 2000, and accepted in revised form July 25, 2000

Recent reports have demonstrated that trans-splicing ribozymes can be employed to repair mutant RNAs. One key factor that influences RNA repair efficiency is the accessibility of the substrate RNA for ribozyme binding, which is complicated by the fact that RNAs may assume multiple conformations and have proteins bound to them *in vivo*. Here we describe a strategy to map accessible sites on sickle  $\beta$ -globin ( $\beta^s$ -globin) transcripts *in vitro* and *in vivo* and to use this information to enhance RNA repair efficiency. Two sites upstream of the sickle mutation were identified as accessible in some fraction of the  $\beta$ -globin RNA by mapping with a ribozyme library and the accessibility of those sites was assessed by *in vitro* cleavage analyses. Ribozymes targeting either site could only convert a certain fraction of the  $\beta^s$ -globin RNA to product but not drive the reaction to completion. However, cleavage and splicing reactions were driven further toward completion when the two ribozymes were both added to the reactions, suggesting that the substrate RNA is present in multiple conformations *in vitro*. These two ribozymes were each able to repair  $\beta^s$ -globin transcripts in erythrocyte precursors derived from peripheral blood from individuals with sickle cell disease. Moreover, the relative accessibility of the targeted sites *in vivo* is as predicted by mapping and *in vitro* analyses. These results demonstrate that this novel RNA mapping strategy represents an effective means to determine the accessible regions of target RNAs and that combinations of trans-splicing ribozymes can be employed to enhance RNA repair efficiency of clinically relevant transcripts such as  $\beta^s$ -globin RNA.

**Key Words:** ribozyme; RNA mapping; RNA repair; sickle cell disease.

## INTRODUCTION

Since the discovery of catalytic RNA molecules, considerable progress has been made in their application as therapeutic agents. Trans-cleaving ribozymes can be employed to cut and thus inactivate a specific deleterious messenger RNA (mRNA) such as those expressed from HIV genes or dominant mutant oncogenes (1–3), while trans-splicing ribozymes can be employed to emend defective transcripts to make them encode a wild

type version of a gene product (4–6). For desired phenotypic changes to be observed in the clinic, the ribozymes must be able to react with a therapeutically relevant fraction of their target RNAs inside a patient's cell. For a cleaving ribozyme to revert neoplastic transformation resulting from a mutation in a dominant oncogene or to inhibit HIV replication, the ribozyme will most likely have to destroy the vast majority of the target transcripts, which may be very difficult to achieve in practice. The minimum efficiency required to engender a phenotypic change by ribozyme-mediated repair of RNA depends on whether the target transcript encodes a dominant or recessive mutant protein. An effective treatment for sickle cell disease would likely result from conversion of 10–20% of  $\beta^s$ -globin transcripts into mRNAs encoding the anti-sickling protein  $\gamma$ -globin (7).

<sup>1</sup>Current address: Department of Molecular Biology, Dankook University, Seoul, Korea.

<sup>2</sup>To whom correspondence should be addressed. E-mail: b.sullenger@cgct.duke.edu.

Trans-splicing of up to 50% of a model *lacZ* substrate RNA has been observed in mammalian cells (8). The repair efficiency of clinically important transcripts in therapeutically appropriate settings however appears to be much lower (5). Thus, improvements in efficiency are likely to be required for ribozyme-mediated RNA repair to become an effective therapeutic strategy. Factors that affect *in vivo* repair efficiency include the accumulation of the ribozyme, colocalization of ribozyme and its target and the proper folding or sequestration of the ribozyme. One key factor that will likely limit the maximum efficiency with which a target RNA can be repaired is the accessibility of the substrate RNA (8, 9). Theoretically the *Tetrahymena* group I ribozyme can be made to target virtually any uridine residue in a substrate RNA by changing the nucleotide composition of the ribozyme's internal guide sequence (IGS) to make it complementary to the target. Within the cell, however, the substrate RNA is presumably in a highly folded structure and may also be protected by proteins bound to part of the molecule. Therefore, it is crucial to first identify the sites within the target RNA that are most accessible to the ribozyme. Toward this end, various strategies have been reported to map the target RNA for accessible binding sites in cell extracts (10, 11).

Previously, we have developed an RNA mapping strategy that is based on a trans-splicing ribozyme library and RNA tagging (5, 12), which can be employed to map ribozyme-accessible sites *in vitro* as well as *in vivo*. In the current study, we use this mapping strategy to identify five uridine residues in the  $\beta$ -globin transcript upstream of the sickle mutation that are accessible to the *Tetrahymena* group I ribozyme. The relative accessibility of these sites was directly measured by *in vitro* cleavage analyses. To determine if repair efficiency can be enhanced by employing multiple ribozymes targeting different sites on one substrate, we chose to study ribozymes targeting the two most accessible sites in the  $\beta$ -globin transcript that we identified by mapping. By combining these ribozymes, we found that cleavage and trans-splicing efficiency appear to be partially additive *in vitro*. In addition, these two ribozymes were each able to convert  $\beta^s$ -globin transcripts into mRNAs encoding  $\gamma$ -globin in erythrocyte precursors derived from peripheral blood from individuals with sickle cell disease. Moreover, the relative efficiency of  $\beta^s$ -globin revision achieved by these two ribozymes was found to be consistent with results from our *in vitro* reactions and mapping studies. Our results suggest that repair efficiency may be enhanced by mapping accessible sites on a target RNA and by combining ribozymes that recognize different accessible sites in a substrate RNA.

## MATERIALS AND METHODS

**Mapping the  $\beta$ -globin transcript.** The mapping library was generated as previously described (5). For *in vitro* mapping, the ribozyme library (500 nM) and cellular RNA (1  $\mu$ g) extracted from erythrocyte precursors derived from umbilical cord blood (UCB) were each denatured at 95°C for 1 min

and then equilibrated in reaction buffer (50 mM Hepes, pH 7.0, 150 mM NaCl, and 5 mM MgCl<sub>2</sub>) at 37°C for 3 min. UCB RNA was then added to the ribozyme library along with guanosine (100  $\mu$ M) to start the reaction, which proceeded at 37°C for 3 h. For intracellular mapping, the ribozyme library was transfected into erythrocyte precursors derived from UCB and total RNA was isolated as previously described (5). The resulting RNA was reverse-transcribed at 37°C for 15 min in the presence of L-argininamide (10 mM) (3' tag primer: 5'-GGGGAATTCGCTATTACGCCAGCTGGCG). cDNAs were then amplified via polymerase chain reaction (PCR) for 30 cycles using the same 3' primer and a 5' primer specific for  $\beta$ -globin (5'-GGGGATCCCTGTGTTCACTAGCAACC). The PCR products were digested with *Bam*HI and *Eco*RI and subcloned into pUC19. Inserts were sequenced using the dideoxy method and the M13 reverse primer (Amersham).

**Plasmid construction.** pT7R61 and pT7R68 were derived from pT7L-21 (13) by oligo cloning. The wild-type group I intron IGS GGAGGG in pT7L-21 was changed to GGGTGC in pT7R61 and to GGGAGT in pT7R68. Plasmids containing the inactive intron were constructed in parallel to provide negative controls for catalytic activity.

pT7R61G was constructed by replacing the *lacZ* sequences in the 3' exon of pT7R61 with human  $\gamma$ -globin cDNA sequence (nucleotides 29 to 545) (14). pT7R68G was constructed by replacing the *lacZ* sequences in the 3' exon of pT7R68 with human  $\gamma$ -globin cDNA sequence (nucleotides 36 to 545) (14). The human  $\gamma$ -globin cDNA sequence was amplified via reverse transcription and polymerase chain reaction (RT/PCR) from total RNA isolated from erythrocyte precursors derived from UCB. One microgram of UCB RNA was reverse transcribed with MoMLV reverse transcriptase at 37°C for 30 min from a primer complementary to human  $\gamma$ -globin cDNA sequence (nucleotides 526 to 545) followed by a *Pst*I site (5'-AAAACGACAGATCTCTTAGCAGAATAGA). The resulting cDNAs were PCR amplified for 30 cycles using this 3' primer as well as a 5' primer (human  $\gamma$ -globin cDNA nt 29–49, 5'-CACAGAGGAGGACAAGGCTAC for pT7R61G; human  $\gamma$ -globin cDNA nt 36–55, 5'-GAGGACAAGGCTACTATCAC for pT7R68G). The PCR products were digested with *Pst*I and inserted between the *Nru*I and *Pst*I sites of pT7R61G and pT7R68G, respectively. Again constructs carrying a catalytically inactive form of the ribozyme were generated in parallel to serve as controls.

**Transcription of ribozymes and substrates.** Rib61ScaI, Rib68ScaI, Rib38ScaI, and Rib52ScaI ribozymes were transcribed using templates generated from plasmid pT7L-21 by PCR. The 5' PCR primers (5'-GGGGGAATTCCTAATACGACTCACTATAGGGTGCAAAAGTTATCAGGC for Rib61ScaI; 5'-GGGGGAATTCCTAATACGACTCACTATAGGGGAGTAAAAGTTATCAGGC for Rib68ScaI, 5'-GGGGGAATTCCTAATACGACTCACTATAGGGTTGAAAAGTTATCAGGC for Rib38ScaI; 5'-GGGGGAATTCCTAATACGACTCACTATAGTGGTGAAAAGTTATCAGGC for Rib52ScaI) contain the T7 promoter and the various ribozymes' internal guide sequences. The 3' primer (5'-ACTCCAAAATAATCAATATAC) is complementary to the last 22 nucleotides of the intron, ending with the *Sca*I site.  $\beta^s$ -Globin RNA was transcribed using a template generated by RT-PCR amplification of RNA from peripheral blood cells from patients with sickle cell disease (upstream primer 5'-GGGGGATCCCTAATACGACTCACTATAGGGACATTTGCTTCTGACACAAC; downstream primer 5'-GGGGGTCGACGCAATGAAAATAATGTTTT). RT-PCR conditions were as described above. PCR products were phenol extracted and ethanol precipitated. Transcription conditions were 40 mM Tris (pH 7.5), 25 mM MgCl<sub>2</sub>, 2 mM spermidine, 10 mM dithiothreitol, 4 mM each nucleoside triphosphate, 500 units T7 RNA polymerase and 1  $\mu$ g PCR product as template per 100- $\mu$ l volume. The resulting RNA was purified on 4% denaturing polyacrylamide gels, eluted overnight at 4°C by soaking the gel slices in buffer (10 mM Tris, pH 7.5, 1 mM EDTA, 0.3 M sodium acetate), and ethanol precipitated. RNA concentrations were determined by measuring the OD<sub>260</sub>, assuming 1 OD<sub>260</sub> = 40  $\mu$ g/ml.  $\beta^s$ -Globin RNA was 5' end labeled using T4 polynucleotide kinase and a molar excess of [ $\gamma$ -<sup>32</sup>P]ATP (6000 Ci/mmol). Rib61-3' $\gamma$ 38 and Rib68-3' $\gamma$ 38 were transcribed using templates generated from plasmids pT7R61G and pT7R68G via PCR amplification. The 3' primer (5'-CCCACAGGCTTGATAG) is complementary to human  $\gamma$ -globin cDNA sequence (nucleotides 49 to 66). Transcription conditions were as described above for *Sca*I ribozymes and  $\beta^s$ -globin RNA, except that the MgCl<sub>2</sub> concentration was lowered to 5 mM to prevent 3' splice site hydrolysis (15). Rib61-3' $\gamma$  and Rib68-3' $\gamma$  were

transcribed from plasmid pT7R61G and pT7R68G, respectively, linearized with *Pst*I. Transcription conditions were as described above for Rib61-3'γ38, except that 10 μg linearized plasmid was used as the transcription template in place of PCR products.

**In vitro cleavage and splicing reactions.** All reactions were single turnover, using trace concentrations of 5'-<sup>32</sup>P-labeled β<sup>s</sup>-globin RNA (1 nM final concentration) and ribozyme excess (300 nM unless otherwise indicated). Ribozyme in 5 μl H<sub>2</sub>O and substrate in 4 μl H<sub>2</sub>O were heated to 95°C for one minute, then renatured at 50°C for 10 min, followed by addition of 5 μl reaction buffer (100 mM Hepes pH 7.0, 300 mM NaCl, 10 mM MgCl<sub>2</sub>) to the ribozyme and substrate, respectively, and 1 μl 2 mM GTP to the substrate. The ribozyme and substrate RNA were incubated at 37°C for 10 min before the reaction was initiated by adding the

substrate to the ribozyme. Reactions were performed at 37°C. Time points were taken by removing 4-μl aliquots and adding them to 4 μl stop solution (90 mM EDTA, 0.05% bromophenol blue, 0.05% xylene cyanol in 88% formamide). Products were separated on 8% denaturing polyacrylamide gels and quantified using a Storm Imager (Molecular Dynamics).

**Pulse-chase experiments.** Cleavage reactions were performed as described above, with 5'-<sup>32</sup>P-labeled β<sup>s</sup>-globin (1 nM) and Rib68ScaI (300 nM) (or Rib61ScaI). After 180 min, the reaction was divided into two equal halves. Fresh buffer and Rib61ScaI (or Rib68ScaI) was added to one half of the reaction so that the final condition was 0.5 nM β<sup>s</sup>-globin RNA, Rib68ScaI (150 nM) and Rib61ScaI (150 nM) in 1× buffer (50 mM Hepes, pH 7.0, 150 mM NaCl, 5 mM MgCl<sub>2</sub>, 0.1 mM GTP). An equal amount of

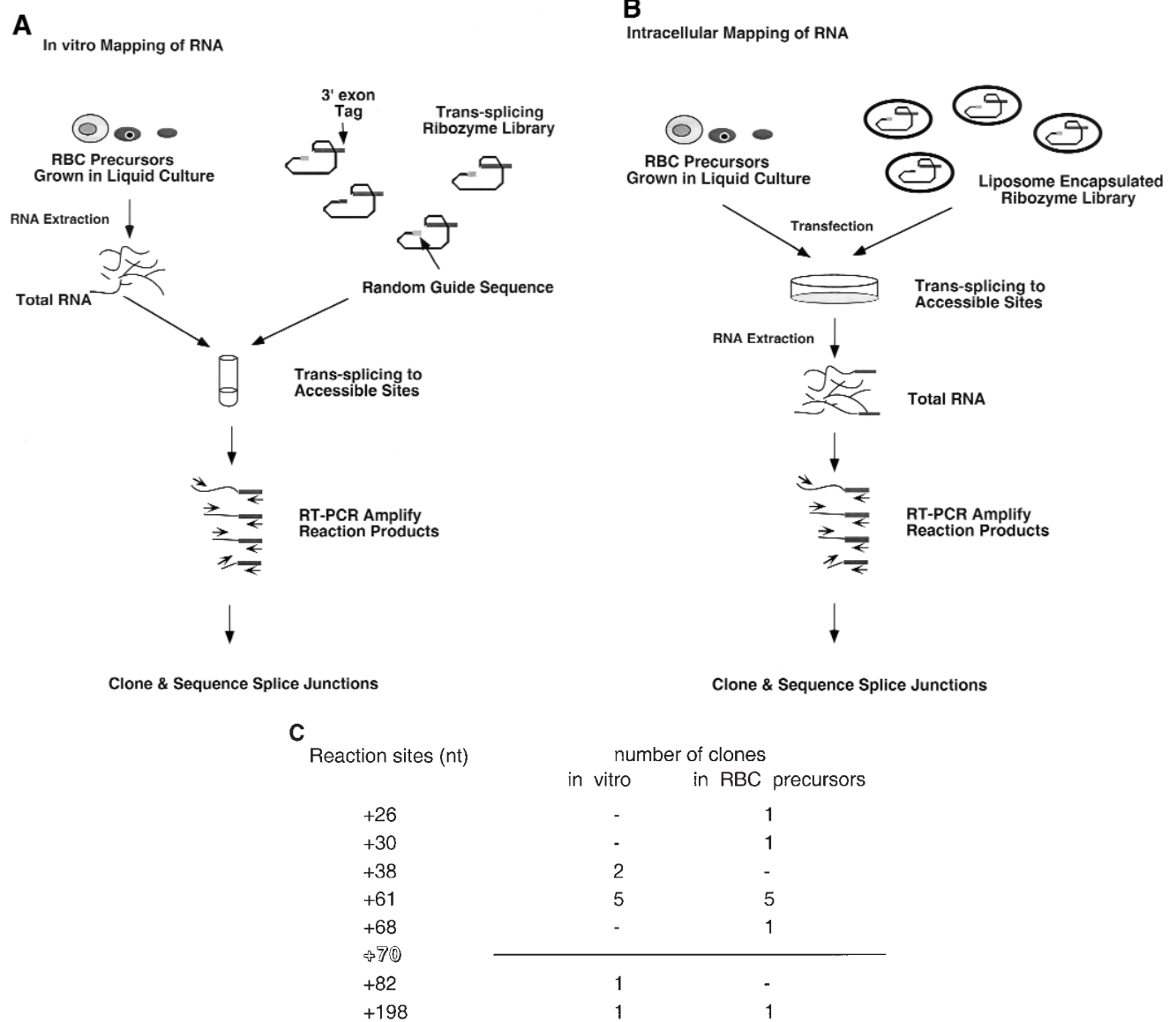
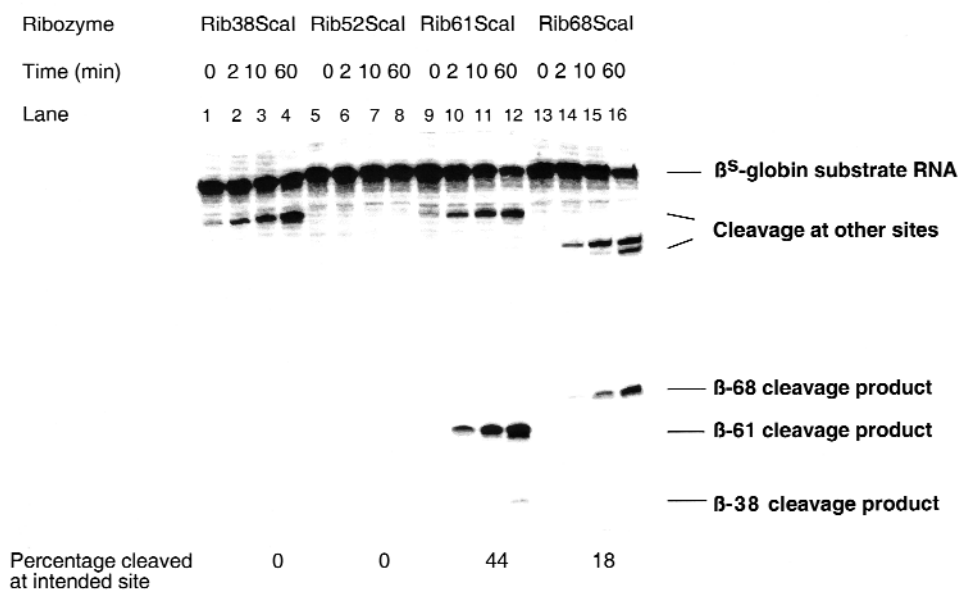


FIG. 1. Mapping of β-globin RNA. (A) Scheme for mapping accessible sites in β-globin RNA *in vitro* with a trans-splicing ribozyme library. (B) Scheme for mapping accessible sites in β-globin RNA in erythrocyte precursors. (C) Mapping results. Nucleotide positions are presented for the accessible uridines identified from *in vitro* (left) and *in vivo* (right) mapping analyses. The number of individual clones containing a given uridine at the splice site is indicated. Position 70 denotes the nucleotide that is altered in β<sup>s</sup>-globin transcripts.



**FIG. 2.** Comparison of accessibility of different sites in  $\beta$ -globin RNA by *in vitro* cleavage analyses.  $\beta$ -Globin substrate RNA was incubated with the four different ribozymes as described under Materials and Methods. Time points were taken and reaction products were separated on an 8% denaturing polyacrylamide gel and visualized and quantified by phosphorimager analysis. The full-length  $\beta$ -globin substrate and the expected cleavage products are indicated along with percent of cleavage at each site after 1 h. Rib61ScaI, Rib38ScaI, and Rib68ScaI cleave  $\beta$ -globin RNA at other positions, which is likely due to the low *in vitro* specificity of group I intron ribozymes (9).

buffer and Rib68ScaI (or Rib61ScaI) were added to the other half of the reaction to serve as a control.

**Isolation and sequencing of spliced products.** RBC precursors derived from peripheral blood from sickle cell patients were transfected with ribozymes and total RNA was isolated as previously described (5). Total RNA were reverse-transcribed at 37°C for 15 min in the presence of L-argininamide (10 mM) (3' tag primer: 5'-CGCTATTACGCCAGCTGGCG; 3'  $\gamma$ -globin primer: 5'-CGGGAATCCACAGGCTTGATA). cDNAs were then amplified for 30 cycles using the same 3' primer and a 5' primer specific for  $\beta$ -globin (5' GGGGATCCCTGTGTTCACTAGCAACC). One microliter of the PCR product was amplified for 30 cycles with the same 5' primer and a nested 3' primer (3' tag primer: 5'-TCGACTCTA-GAGGATCCC; 3'  $\gamma$ -globin primer: 5' CGGGAATTCGTGATAGTAGC-CTTGTCCT). [ $\alpha$ -<sup>32</sup>P]dCTP was added to second round PCR to label the amplified products which were separated on a 10% polyacrylamide gel and quantified using a Storm Imager (Molecular Dynamics).

The PCR products from Rib-3'  $\gamma$  were digested with *Bam*HI and *Eco*RI and subcloned into pUC19. Inserts were sequenced using the dideoxy method and the M13 reverse primer (Amersham).

## RESULTS

**Mapping  $\beta$ -globin RNA for accessible uridines.** To ascertain which regions of the  $\beta$ -globin transcript are accessible to ribozymes, we developed an RNA mapping strategy that is based on a trans-splicing ribozyme library and RNA tagging (12) (Figs. 1A and 1B). The mapping library was generated by randomizing the guide sequence of the *Tetrahymena* group I trans-splicing ribozyme such that the 5' end of the RNAs in the library began with 5'-GNNNNN-3' where "G" represents guanine and "N" represents equal amounts of the four nucleotides (16). The  $\beta$ -globin transcript was mapped *in vitro* by incubating the

trans-splicing ribozyme library with total RNA isolated from erythrocyte precursors under splicing conditions (Fig. 1A) and inside the cell by transfecting the mapping library into erythrocyte precursors (Fig. 1B). Mapping studies revealed five uridine residues upstream of the sickle mutation in  $\beta$ -globin RNA (position 70) to be accessible to a group I intron ribozyme (Fig. 1C). Moreover, the uridine at position 61 (U61) appears to be particularly accessible with more than half of the reaction products resulting from splicing at this site (Fig. 1C).

**Verifying that RNA mapping predicts the most accessible sites *in vitro*.** To determine if the sites that are predicted to be accessible via mapping analyses are truly the most accessible sites, we decided to analyze in more detail ribozymes targeting three different sites in  $\beta$ -globin RNA that were identified by our mapping studies. U61 appeared to be particularly accessible because ten out of eighteen clones generated during *in vitro* and intracellular mapping contained splice junctions at this nucleotide (Fig. 1C). Splicing at nucleotides 38 (U38) and 68 (U68) was observed in one or two clones out of eighteen, while splicing at nucleotide 52 (U52) was not detected in our mapping analyses (Fig. 1C). Trans-cleaving group I ribozymes were designed to recognize these individual sites (called Rib61ScaI, Rib38ScaI, Rib68ScaI, and Rib52ScaI). These cleaving ribozymes catalyze only the first step of splicing (cleavage) and not exon ligation due to their lack of a 3' exon and a 3' terminal guanosine (13, 17). Therefore the percentage of cleavage product generated by the individual ribozymes is a direct meas-

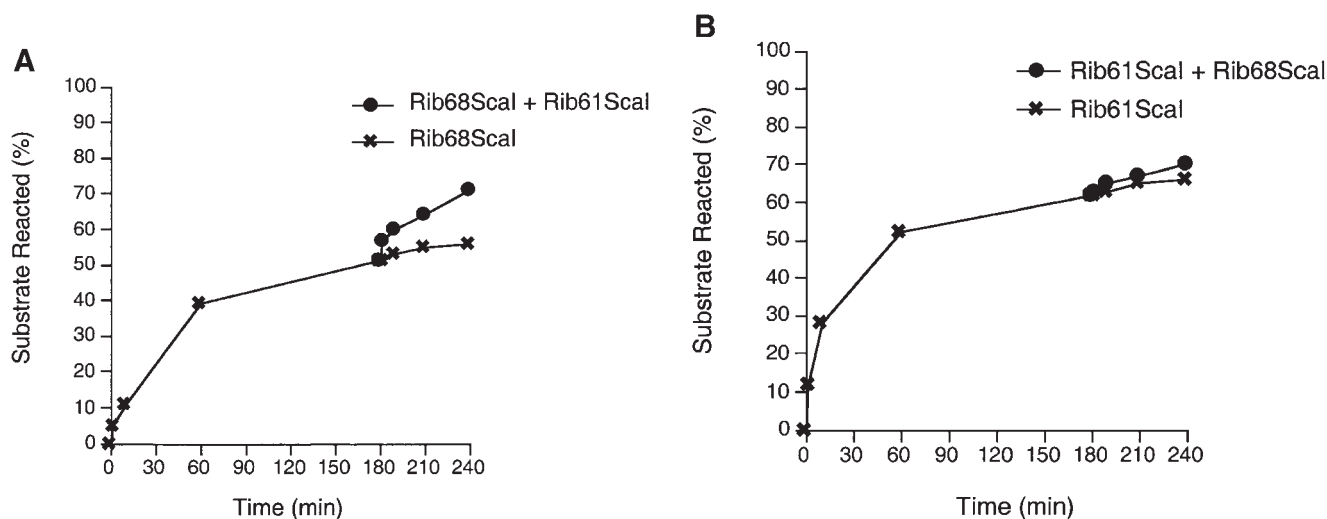


FIG. 3. Chasing ribozyme reactions toward completion. Radiolabeled  $\beta$ -globin RNA was incubated with either (A) Rib68ScaI or (B) Rib61ScaI and time points were taken at 0, 2, 10, 60, and 180 min. After 180 min, more of the starting ribozyme was added to half of the sample, while (A) Rib61ScaI or (B) Rib68ScaI was added to the other half of the reaction. Aliquots were removed and the reactions stopped at times of 182, 190, 210, and 240 min. All reaction products were separated on an 8% denaturing polyacrylamide gel and quantified using a phosphorimager.

ure of the accessibility of the uridine residue being targeted.

In single turnover reactions, Rib61ScaI (Fig. 2, lanes 9–12) cleaved  $\beta$ -globin RNA at U61 with higher efficiency than Rib68ScaI (Fig. 2, lanes 13–16) cleaved the target RNA at U68. Moreover, Rib52ScaI (Fig. 2, lanes 5–8) and Rib38ScaI (Fig. 2, lanes 1–4) did not generate cleavage products at the expected sites, indicating that U38 and U52 in full-length  $\beta$ -globin RNA were inaccessible to the ribozyme. Similarly the inactive versions of all four ribozymes were unable to cleave  $\beta$ -globin RNA (data not shown). Interestingly however, Rib61ScaI generated a cleavage product that corresponds in length to  $\beta$ -globin RNA cleaved at U38 at later time points (Fig. 2, lane 12). One possible explanation for this miscleavage is that while U38 in full-length  $\beta$ -globin RNA is not accessible, after  $\beta$ -globin RNA is cut at U61, this cleavage product folds into a different conformation that allows U38 to become accessible to Rib61, whose guide sequence (GGGUGC) can bind to the U38 site (CAACCT) with a two-nucleotide mismatch. The relative cleavage efficiency of  $\beta$ -globin at these four sites corresponds with the predicted accessibility from our mapping analyses. Moreover, the site that was most frequently represented in the reaction products generated during mapping (U61) appears to be the most accessible site for cleavage *in vitro*.

**Enhancing reaction efficiency by using a combination of ribozymes.** When trace amounts of  $5'$ - $^{32}$ P-labeled  $\beta$ -globin RNA were allowed to react with an excess of Rib68ScaI for 3 h, approximately 50% of the substrate remained uncleaved (Fig. 3A). Prolonged incubation with or addition of more Rib68ScaI failed to drive the reaction much further toward completion (Fig. 3A, curve

with X). One possible explanation for Rib68's inability to cleave all of the substrate is that  $\beta$ -globin RNA may assume multiple folded structures with certain conformations allowing Rib68 access to U68 and others not. To determine if a second ribozyme could react with any of the substrate that is inaccessible to Rib68, we incubated  $5'$ - $^{32}$ P-labeled  $\beta$ -globin RNA with an excess of Rib68ScaI for 3 h and then added Rib61ScaI to the reaction. A significant proportion of substrate previously inaccessible to Rib68ScaI was cleaved by Rib61ScaI (Fig. 3A, curve with ●), whereas the addition of Rib68ScaI did not significantly cleave any more of the substrate (Fig. 3A, curve with X). This observation suggests that a portion of the  $\beta$ -globin transcripts that are inaccessible to Rib68ScaI are accessible to Rib61ScaI. When Rib68ScaI was added to a stalled reaction containing Rib61ScaI (Fig. 3B), the effect was less dramatic in that Rib61ScaI is more effective than Rib68ScaI and drives the reaction further toward completion by itself. These results suggest that at least three conformations for  $\beta$ -globin RNA coexist: one that is accessible to only Rib61ScaI, a second that is accessible to both Rib61ScaI and Rib68ScaI, and a third that allows neither Rib61ScaI nor Rib68ScaI access. A small fraction of  $\beta$ -globin RNAs that assume a fourth conformation that is accessible to only Rib68ScaI may also be present.

Since a portion of the  $\beta$ -globin transcripts that are inaccessible to Rib68ScaI appear to be accessible to Rib61ScaI, a combination of the two ribozymes may cleave the substrate RNA to a greater extent in a given amount of time than either ribozyme alone. To test this possibility, we incubated  $5'$ - $^{32}$ P-labeled  $\beta$ -globin RNA with Rib61ScaI alone, Rib68ScaI alone or with both Rib61ScaI and Rib68ScaI and measured the rate and

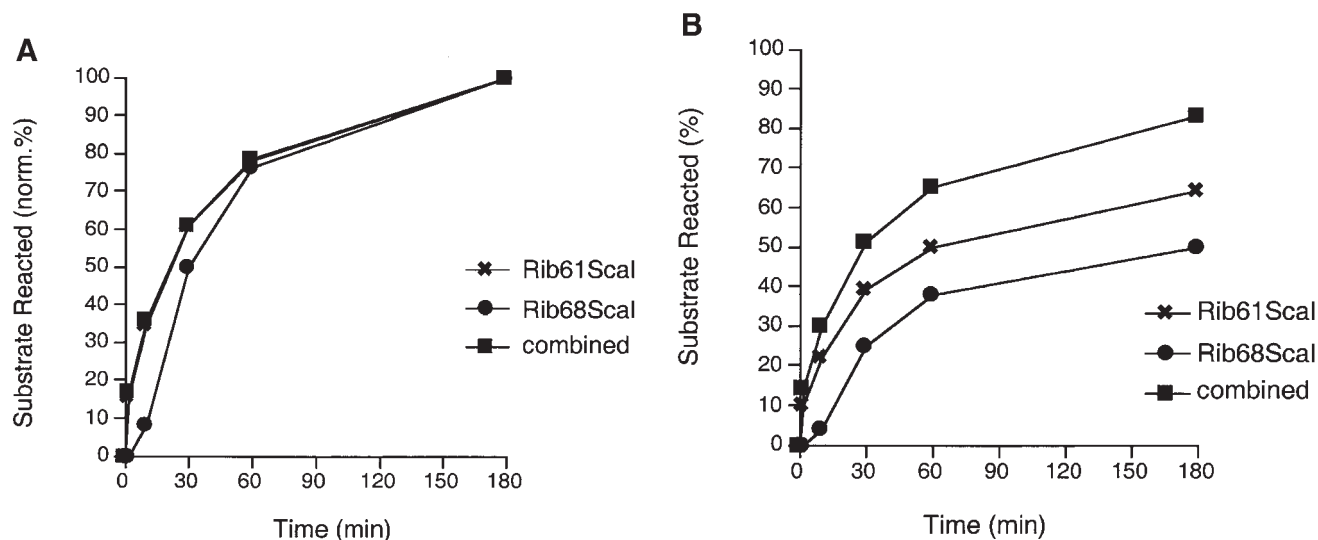


**FIG. 4.** Enhancing substrate cleavage efficiency by using two ribozymes. 5'-<sup>32</sup>P-labeled  $\beta$ -globin RNA (1 nM) was incubated with Rib68Scal (300 nM) (●), Rib61Scal (300 nM) (X) and both Rib61Scal (150 nM) and Rib68Scal (150 nM) (○). Time points were taken at 0, 2, 10, 60, and 180 min and reaction products were separated on an 8% denaturing polyacrylamide gel and quantified. The percentage of substrate reacted is plotted against time. B shows the absolute values for the *in vitro* cleavage reactions, while in Part A data have been normalized for each reaction in B such that the fraction cleaved (norm.) is equal to the fraction cleaved at each time point divided by the maximum fraction cleaved during the reaction.

extent of substrate cleavage. The two ribozymes appeared to cleave the substrate at similar rates, alone (Fig. 4A, curves with ● and X) or when they are combined (Fig. 4A, curve with ■). However, the extent of  $\beta$ -globin RNA cleavage observed when using the combination of two ribozymes (Fig. 4B, curve with ■) is significantly greater than the cleavage efficiency obtained by the individual ribozymes (Fig. 4B, curves with ● and X).

To determine if trans-splicing reaction efficiency can also be enhanced by combining ribozymes that target different sites on a substrate RNA, we incubated 5'-<sup>32</sup>P-labeled  $\beta$ -globin RNA with Rib61-3' $\gamma$ 38, Rib68-3' $\gamma$ 38, or with a combination of these two ribozymes that contain a 3' exon derived from human  $\gamma$ -globin sequences, and measured the rate and extent of these trans-splicing reactions. As with the cleavage reactions, the rate of trans-splicing is

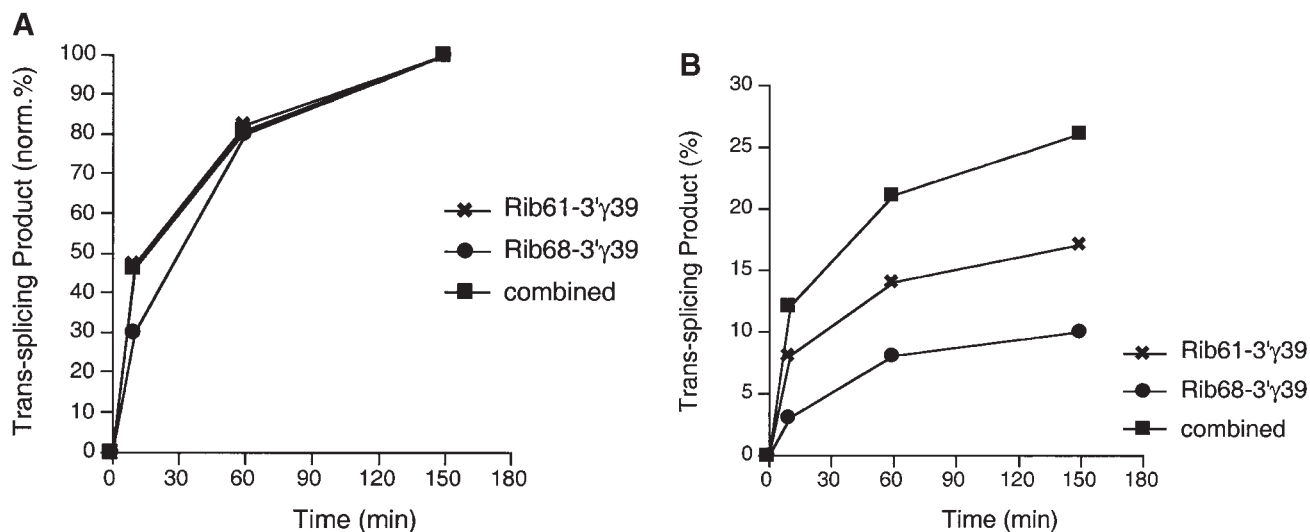


**FIG. 5.** Enhancing substrate splicing efficiency by using two ribozymes. 5'-<sup>32</sup>P-labeled  $\beta$ -globin (1 nM) was incubated with Rib68-3' $\gamma$ 38 (500 nM) (●), Rib61-3' $\gamma$ 38 (500 nM) (X) and both Rib61-3' $\gamma$ 38 (250 nM) and Rib68-3' $\gamma$ 38 (250 nM) (○). Time points were taken at 0, 2, 10, 60, and 180 min and reaction products were separated on an 8% denaturing polyacrylamide gel and quantified. The percentage of splicing product is plotted against time. B shows the absolute values for the *in vitro* trans-splicing reactions, while in A data have been normalized for each reaction in B such that the fraction spliced (norm.) is equal to the fraction spliced at each time point divided by the maximum fraction spliced during the reaction.

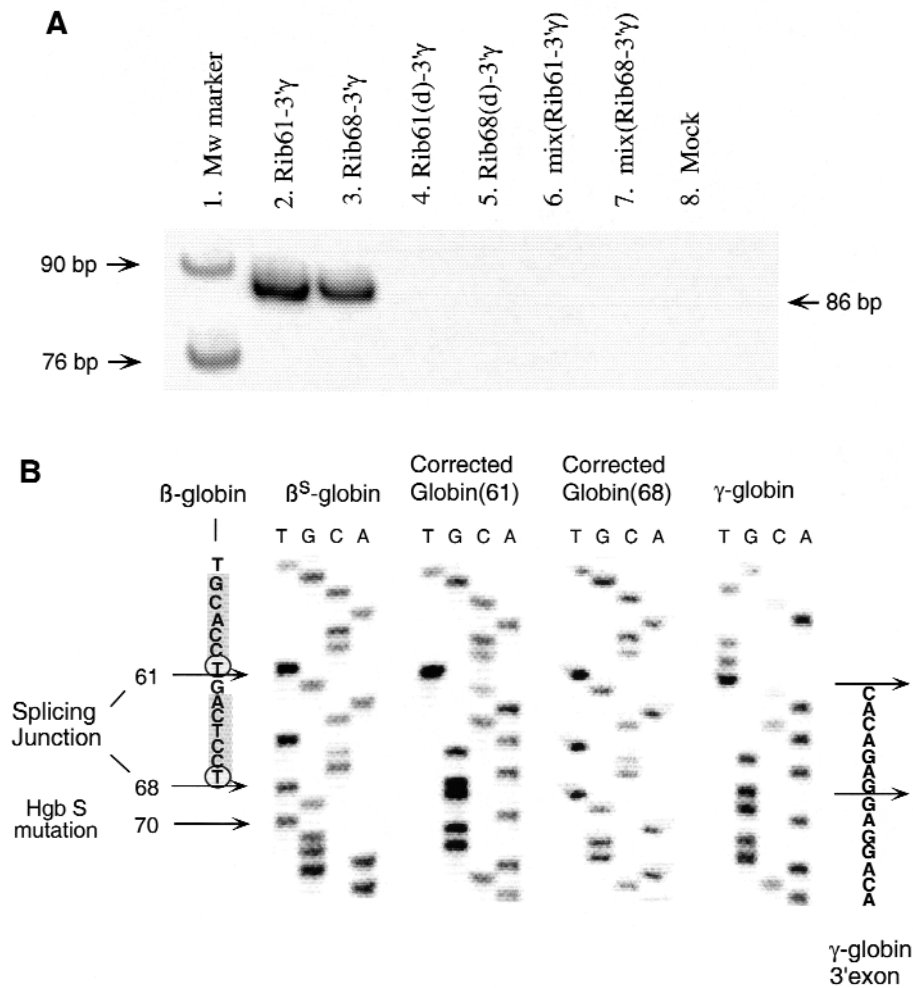


FIG. 6. Converting  $\beta$ -globin transcripts into  $\gamma$ -globin encoding RNAs in erythrocyte precursors from peripheral blood of sickle cell patients. (A) RT-PCR analysis of amended  $\beta$ -globin RNAs. The migration of the expected PCR products of 86 base pairs as well as molecular weight markers of 90 and 70 base pairs are indicated. (B) Sequence of amended globin transcripts. The expected sequence for a corrected transcript around the splicing junction is shown, with the complement to the two IGSs shaded and the uridines at position 61 and 68 circled.  $\beta$ -Globin and  $\gamma$ -globin sequences are provided for comparison and the mutant nucleotide in the sickle  $\beta$ -globin transcript indicated.

similar in each case (Fig. 5A) while the extent of trans-splicing when using two ribozymes is significantly increased and partially additive compared to reactions with individual ribozymes (Fig. 5B). These results are consistent with the hypothesis that the  $\beta$ -globin RNA assumes multiple conformations that allow different ribozymes access to various fractions of the folded substrate. Moreover, these results indicate that combining ribozymes targeting different sites on the  $\beta$ -globin RNA is an effective way of increasing trans-splicing reaction efficiency.

In the cleavage reaction containing both Rib61 and Rib68, approximately 80% of the substrate RNA was cleaved by 180 min (Fig. 4B, curve with ■). By contrast, in the trans-splicing reaction containing both ribozymes, only 25% of substrate RNA was converted into splice product by 180 min (Fig. 5B, curve with ■). This difference in reaction efficiency is not unexpected in that the

second step of the splicing reaction appears to be reversible. Thus, an equilibrium exists in which only a fraction of cleavage intermediate is converted to ligated product (18, 19).

*Rib61-3'γ and Rib68-3'γ can each repair β-globin transcripts in erythrocyte precursors.* We have previously shown that a trans-splicing ribozyme targeting U61 in  $\beta$ -globin RNA could convert  $\beta$ -globin transcripts into mRNAs encoding  $\gamma$ -globin in a clinically relevant cellular context (5). To determine whether a trans-splicing ribozyme targeting U68 could repair  $\beta$ -globin transcripts in erythrocyte precursors as well, we created Rib68-3'γ, which contains human  $\gamma$ -globin mRNA sequence (nucleotides 36–545) as a 3' exon. Rib61-3'γ and Rib68-3'γ were each transfected into erythrocyte precursors derived from sickle cell patients. Trans-spliced products were detected in total RNA isolated from these cells using RT/PCR amplification. A DNA fragment of the expected size (86 base

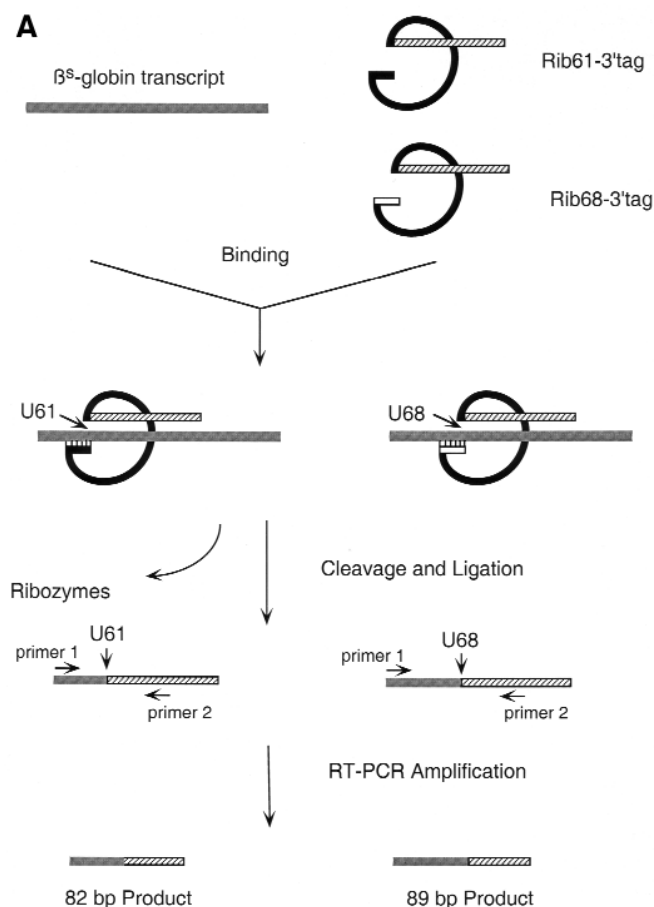
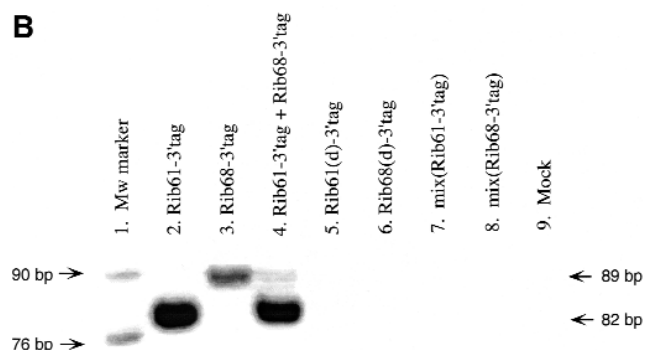


**FIG. 7.** Assessing the relative trans-splicing efficiency of Rib61 and Rib68 in erythrocyte precursors by competitive RT-PCR. The migration of PCR products of 82 (Rib61-3'tag) and 89 (Rib68-3'tag) base pairs and molecular weight markers of 90 and 76 base pairs are indicated.



pairs) was generated when analyzing RNA from cells transfected with Rib61-3' $\gamma$  or Rib68-3' $\gamma$  (Fig. 6A, lanes 2 and 3). No such product was generated from RNA samples isolated from cells that were not transfected (Fig. 6A, lane 8) or were transfected with the inactive ribozymes (Fig. 6A, lanes 4 and 5). When Rib61-3' $\gamma$  or Rib68-3' $\gamma$  was added to the RNA extraction buffer used to isolate total RNA from a sample of mock-transfected erythrocyte precursors, no amplification product was generated (Fig. 6A, lanes 6 and 7), suggesting that the observed trans-splicing products were generated inside the RBC precursors and not during lysis of the cells or RNA analysis.

Sequence analysis of four different subclones each derived from sickle cell patient samples transfected with Rib61-3' $\gamma$  or Rib68-3' $\gamma$  demonstrated that in each case the ribozyme had correctly spliced its  $\gamma$ -globin 3' exon onto the intended nucleotide of the  $\beta^s$ -globin target transcript and in the process maintained the open reading frame for the translation of the mRNA (Fig. 6B). Thus, Rib68-3' $\gamma$  as well as Rib61-3' $\gamma$  is able to correct mutant globin transcripts in primary human RBC precursors with high fidelity.

*Evaluating the accessibility of U61 and U68 in  $\beta^s$ -globin RNA inside erythrocyte precursors.* To determine if the relative accessibility of U61 and U68 *in vivo* is similar to

their relative accessibility *in vitro*, we generated two ribozymes, Rib61-3'tag and Rib68-3'tag, that contain identical 3' exon tag sequences. The trans-splicing products generated by these two ribozymes are expected to differ in size by seven nucleotides due to the difference in the length of their 5' exons following splicing. The two ribozymes were transfected individually and together into erythrocyte precursors derived from sickle cell patients. Trans-spliced products were detected in total RNA from transfected cells by RT/PCR amplification (Fig. 7). Amplified fragments of the expected size (82 base pairs from Rib61-3'tag and 89 base pairs from Rib68-3'tag) were obtained when analyzing the RNA samples isolated from cells that were transfected with Rib61-3'tag (Fig. 7, lane 2) and Rib68-3'tag (Fig. 7, lane 3), respectively. Two distinct bands were detected from the RNA samples isolated from cells that were transfected with equal amounts of Rib61-3'tag and Rib68-3'tag (Fig. 7, lane 4). Trans-splicing products generated by Rib61-3'tag constitute approximately 90% of the total spliced products found in these cells, while products generated by Rib68-3'tag account for only 10% of the total products. By contrast no such product was generated from RNA samples isolated from cells that were not transfected (Fig. 7, lane 9) or were transfected with the inactive



ribozymes (Fig. 7, lanes 5 and 6). Moreover, no amplification product was generated from RNA samples in which Rib61-3'tag or Rib68-3'tag was added to the RNA extraction buffer prior to lysing the mock transfected cells (Fig. 7, lanes 7 and 8). These results indicate that U61 is more accessible than U68 on  $\beta^s$ -globin transcripts in cells from sickle patients as our *in vivo* mapping analysis predicted.

## DISCUSSION

In this report, the uridine residues in the human  $\beta$ -globin transcript that are accessible to trans-splicing ribozymes were ascertained by an RNA mapping strategy based on a group I ribozyme library and RNA tagging (12) (Fig. 1). To validate that this novel RNA mapping approach identifies accessible sites, the relative accessibility of individual uridine residues was assessed by *in vitro* cleavage analyses (Fig. 2). Results from these studies indicate that RNA mapping does yield the identity of ribozyme accessible sites on substrate RNAs and that such mapping can provide information about the relative accessibility of the identified sites. Moreover, combining ribozymes targeting two different accessible sites on the  $\beta^s$ -globin RNA enhanced cleavage (Figs. 3 and 4) and splicing (Fig. 5) efficiency of the substrate. Finally, these two ribozymes were each able to convert the  $\beta^s$ -globin transcripts into mRNAs encoding  $\gamma$ -globin in erythrocyte precursors derived from peripheral blood from sickle patients with high fidelity (Fig. 6) and the relative intracellular accessibility of the two targeted sites was as predicted from *in vivo* mapping analysis (Fig. 7).

The uridine at position 61 of  $\beta$ -globin RNA was identified as being particularly accessible by our mapping studies because over half of the reaction products sequenced contained splice junctions at this nucleotide (Fig. 1C). Nevertheless, RNA mapping is an indirect measure of accessibility and may not be entirely accurate. First, in a competitive PCR-based assay, shorter templates tend to be preferentially amplified over longer templates. The sites close to the upstream primer may therefore be over-represented in the amplified pool. This bias may not pose a serious problem in the mapping of  $\beta^s$ -globin RNA because the mutation of interest is close to the 5'-end of the transcript. However, preferential amplification should be taken into consideration when mapping a longer RNA sequence. For example, recently we mapped accessible sites over several hundred bases on p53 transcripts using the same approach as described herein except that we employed several 5'-PCR primers specific for the p53 sequence that recognized p53 RNA at 200 nucleotide intervals (unpublished data). Second, when ribozymes targeting multiple sites are present in the same reaction cocktail, splicing events may occur in which the 5'-portion of the RNA is spliced again at an upstream site. Therefore, it is possible that some of the sites that were identified as being accessible with mapping analysis may not be accessible in the full-length

transcript but only became accessible after reaction at another downstream site. In this report we directly measured the accessibility of various uridines by *in vitro* cleavage reactions using trans-cleaving group I ribozymes targeting different sites in the  $\beta^s$ -globin transcript (Fig. 2). The results verified that U61 was the most accessible residue among the four sites that were assessed, which was consistent with the results of our *in vitro* mapping analysis. The cleavage at U38 by Rib61 and the failure of Rib38 to cleave at the same site suggest the possibility that some of the sites that were identified in mapping resulted from secondary reactions. Several other sites downstream of the sickle mutation that are likely to have the same or similar nucleotide composition on the 5' end as the intended sites appeared to be effectively cleaved (Fig. 2). The fact that they were not identified in mapping is likely due to preferential amplification of shorter templates.

Cleavage of full-length  $\beta^s$ -globin RNA by Rib68ScaI failed to go to completion after prolonged incubation (Fig. 3A, curve with X), which suggests that  $\beta^s$ -globin transcripts may be assuming multiple conformations such that U68 in a fraction of the substrate molecules is inaccessible to Rib68. The observation that addition of Rib61 to this "stalled" reaction drove a significant fraction of the remaining substrate RNA to product (Fig. 3A, curve with ●) and the similar result where Rib68ScaI was added to Rib61ScaI reaction mixture (Fig. 3B) suggest that  $\beta^s$ -globin transcripts may assume at least four conformations *in vitro* that differentially allow Rib61ScaI and Rib68ScaI access to their target sites. By combining ribozymes that target U61 and U68, we have observed a partially additive effect in the extent of *in vitro* cleavage (Fig. 4B) and splicing reactions (Fig. 5B). The rate of the reactions however were similar for each ribozyme, either alone or combined (Figs. 4A and Fig. 5A). These results are consistent with the hypothesis that different conformations coexist in the substrate. Under single turnover conditions, the extent of the reaction will be largely dictated by the fraction of the substrate that is accessible to a given ribozyme. Each conformation that is open to the ribozyme appears to react at a similar rate. Combining ribozymes that target different conformations of the substrate therefore does not increase the overall reaction rate but rather drives the reaction further toward completion.

Ribozymes must be able to react with a therapeutically significant proportion of their target RNAs inside a patient's cell in order to induce desired phenotypic changes. The maximum percentage of repair efficiency that one ribozyme can achieve will be limited by the fraction of the substrate RNA that assumes a conformation that is accessible to the particular ribozyme. The results from *in vitro* cleavage and splicing assays clearly indicate that by combining ribozymes which react with different conformations of a substrate, the overall accessibility of the substrate can be enhanced and repair efficiency can be improved *in vitro*. Inside the cell, however,

target RNAs may assume completely different folded structures than they do *in vitro* and substrate RNAs may change their conformation during their life spans *in vivo*. Moreover, both the substrate and the ribozyme may be bound by proteins which can act as chaperones that affect RNA folding (20). Interactions between these proteins and either the ribozyme or its substrate may profoundly affect ribozyme activity (21, 22). Nevertheless, although little is known about the actual conformation of large mRNA molecules, a growing body of evidence shows that the folding of mRNA *in vivo* influences a diverse range of biological events such as mRNA splicing (23, 24), processing (25–27), translational control (28–30) and regulation (31–33). Coexisting conformations that result in differences in RNA stability (34, 35), repressed translation (36) or alternative splicing (37) have been reported. It is therefore reasonable to believe that mRNAs may generally assume multiple conformations *in vivo*, which suggests that RNA repair efficiency can be enhanced *in vivo* by combining trans-splicing ribozymes targeting different sites in a mutant mRNA.

When transfected into erythrocyte precursors derived from peripheral blood from sickle patients, both Rib61-3' $\gamma$  and Rib68-3' $\gamma$  were able to convert  $\beta^s$ -globin transcripts into mRNAs encoding the anti-sickling protein  $\gamma$ -globin (Fig. 6). *In vivo* trans-splicing by these two ribozymes indicates that the relative accessibility of U61 and U68 inside the erythrocyte precursors is approximately nine to one (Fig. 7), which is consistent with our *in vivo* mapping analysis that suggests U61 is more accessible than U68 (Fig. 1C). Moreover, in the case of  $\beta^s$ -globin RNA, U61 appears to be more accessible than U68 both *in vitro* and inside cells. It will be interesting to determine if this correlation between *in vitro* and *in vivo* accessibility holds true for other target RNAs.

In conclusion, these studies demonstrate that this novel approach to RNA mapping identifies ribozyme-accessible sites on substrate RNAs *in vitro* as well as *in vivo*. Therefore this approach should be of general utility to a wide range of studies that employ ribozymes or antisense RNAs to modify the activity of target RNAs by binding to them. Mapping analysis appears to yield more than one accessible site. This information can be used to generate multiple ribozymes targeting various accessible sites. The ability to create multiple ribozymes is likely to be particularly important because target RNAs probably assume multiple conformations inside cells, making it necessary to combine ribozymes that target different sites to effectively enhance reaction efficiency. Using the strategies described herein to enhance RNA repair efficiency will greatly facilitate the development of therapeutically useful ribozymes to treat genetic disorders such as sickle cell disease.

#### ACKNOWLEDGMENTS

We thank P. Zarrinkar, C. Rusconi, L. Warner, J. Byun, J. Jones, M. Long, and H. Tian for helpful discussions. This study was supported in part by the Korean Academic Research Fund of the Ministry of Education (KRF-98-019-F00026; S.-

W. L.) and a grant (HL57606) from the National Heart, Lung, and Blood Institute (NHLBI) (B.A.S.).

#### REFERENCES

- Rossi, J. J. (1992). Ribozymes. *Curr. Opin. Biotechnol.* 3: 3–7.
- Sullenger, B. A., and Cech, T. R. (1993). Tethering ribozymes to a retroviral packaging signal for destruction of viral RNA. *Science* 262: 1566–1569.
- Yu, M., Poeschla, E., and Wong-Staal, F. (1994). Progress toward gene therapy for HIV infection. *Gene Ther.* 1: 13–26.
- Sullenger, B. A., and Cech, T. R. (1994). Ribozyme-mediated repair of defective mRNA by targeted trans-splicing. *Nature* 371: 619–622.
- Lan, N., Howrey, R. P., Lee, S.-W., Smith, C. A., and Sullenger, B. A. (1998). Ribozyme mediated repair of sickle  $\beta$ -globin mRNAs in erythrocyte precursors. *Science* 280: 1593–1596.
- Phylactou, L. A., Darrah, C., and Wood, M. J. A. (1998). Ribozyme-mediated trans-splicing of a trinucleotide repeat. *Nat. Genet.* 18: 378–381.
- Powars, D. R., Weiss, J. N., Chan, L. S., and Schroeder, W. A. (1984). Is there a threshold level of fetal hemoglobin that ameliorates morbidity in sickle cell anemia? *Blood* 63: 921–926.
- Jones, J. T., and Sullenger, B. A. (1997). Evaluating and enhancing ribozyme reaction efficiency in mammalian cells. *Nat. Biotechnol.* 15: 902–905.
- Herschlag, D. (1991). Implications of ribozyme kinetics for targeting the cleavage of specific RNA molecules *in vivo*: More isn't always better. *Proc. Natl. Acad. Sci. USA* 88: 6921–6925.
- Mir, K. U., and Southern, E. M. (1999). Determining the influence of structure on hybridization using oligonucleotide arrays. *Nat. Biotechnol.* 17: 788–792.
- Scherr, M., and Rossi, J. J. (1998). Rapid determination and quantitation of the accessibility to native RNAs by antisense oligodeoxynucleotides in murine cell extracts. *Nucleic Acids Res.* 26: 5079–5085.
- Jones, J. T., Lee, S. W., and Sullenger, B. A. (1996). Tagging ribozyme reaction sites to follow trans-splicing in mammalian cells. *Nat. Med.* 2: 643–648.
- Zaug, A. J., Grosshans, C. A., and Cech, T. R. (1988). Sequence-specific endoribonuclease activity of the *Tetrahymena* ribozyme: Enhanced cleavage of certain oligonucleotide substrates that form mismatched ribozyme–substrate complexes. *Biochemistry* 27: 8924–8931.
- Cavallesco, C., et al. (1980). Nucleotide sequence of human  $\gamma$ -globin messenger RNA. *Gene* 12: 215–221.
- Zaug, A. J., McEvoy, M. M., and Cech, T. R. (1993). Self-splicing of the group I intron from *Anabaena* pre-tRNA: Requirement for base-pairing of the exons in the anticodon stem. *Biochemistry* 32: 7946–7953.
- Cambell, T. B., and Cech, T. R. (1995). Identification of ribozymes within a ribozyme library that efficiently cleave a long substrate RNA. *RNA* 1: 598–609.
- Herschlag, D., and Cech, T. R. (1990). Catalysis of RNA cleavage by the *Tetrahymena thermophila* ribozyme. 1. Kinetic description of the reaction of an RNA substrate complementary to the active site. *Biochemistry* 29: 10159–10171.
- Mei, R., and Herschlag, D. (1996). Mechanistic investigations of a ribozyme derived from the *Tetrahymena* group I intron: Insights into catalysis and the second step of self-splicing. *Biochemistry* 35: 5796–5809.
- Zarrinkar, P. P., and Sullenger, B. A. (1998). Probing the interplay between the two steps of group I intron splicing: Competition of exogenous guanosine with omega G. *Biochemistry* 37: 18056–18063.
- Herschlag, D. (1995). RNA chaperones and the RNA folding problem. *J. Biol. Chem.* 270: 20871–20874.
- Bertrand, E. L., and Rossi, J. J. (1994). Facilitation of hammerhead ribozyme catalysis by the nucleocapsid protein of HIV-1 and the heterogeneous nuclear ribonucleoprotein A1. *EMBO J.* 13: 2904–2912.
- Herschlag, D., Khosla, M., Tsuchihashi, Z., and Karpel, R. L. (1994). An RNA chaperone activity of non-specific RNA binding proteins in hammerhead ribozyme catalysis. *EMBO J.* 13: 2913–2924.
- Coleman, T. P., and Roesser, J. R. (1988). RNA secondary structure: An important cis-element in rat calcitonin/CGRP pre-messenger RNA splicing. *Biochemistry* 37: 15941–15950.
- Cote, J., and Chabot, B. (1997). Natural base-pairing interactions between 5' splice site and branch site sequences affect mammalian 5' splice site selection. *RNA* 3: 1248–1261.
- van Gelder, C. W., et al. (1993). A complex secondary structure in U1A pre-mRNA that binds two molecules of U1A protein is required for regulation of polyadenylation. *EMBO J.* 12: 5191–5200.
- Vasserot, A. P., Schaufele, F. J., and Birnstiel, M. L. (1989). Conserved terminal hairpin sequences of histone mRNA precursors are not involved in duplex formation with the U7 RNA but act as a target site for a distinct processing factor. *Proc. Natl. Acad. Sci. USA* 86: 4345–4349.
- Allain, F. H., et al. (1996). Specificity of ribonucleoprotein interaction determined by RNA folding during complex formulation. *Nature* 380: 646–650.
- Wang, C., Sarnow, P., and Siddiqui, A. (1994). A conserved helical element is essential for internal initiation of translation of hepatitis C virus RNA. *J. Virol.* 68: 7301–7307.
- Pelletier, J., and Sonenberg, N. (1987). The involvement of mRNA secondary structure in protein synthesis. *Biochem. Cell Biol.* 65: 576–581.
- Shen, L. X., and Tinoco, I., Jr. (1995). The structure of an RNA pseudoknot that caus-

es efficient frameshifting in mouse mammary tumor virus. *J. Mol. Biol.* 247: 963–978.

<sup>31</sup>Hentze, M. W., *et al.* (1987). Identification of the iron-responsive element for the translational regulation of human ferritin mRNA. *Science* 238: 1570–1573.

<sup>32</sup>Casey, J. L., Koeller, D. M., Ramin, V. C., Klausner, R. D., and Harford, J. B. (1989). Iron regulation of transferrin receptor mRNA levels requires iron-responsive elements and a rapid turnover determinant in the 3' untranslated region of the mRNA. *EMBO J.* 8: 3693–3699.

<sup>33</sup>Adress, K. J., Basilion, J. P., Klausner, R. D., Rouault, T. A., and Pardi, A. (1997). Structure and dynamics of the iron responsive element RNA: Implications for binding of the RNA by iron regulatory binding proteins. *J. Mol. Biol.* 274: 72–83.

<sup>34</sup>Rosenbaum, V., *et al.* (1993). Co-existing structures of an mRNA stability determinant. The 5' region of the *Escherichia coli* and *Serratia marcescens* ompA mRNA. *J. Mol. Biol.* 229: 656–670.

<sup>35</sup>Gluick, T. C., Gerstner, R. B., and Draper, D. E. (1997). Effects of Mg<sup>2+</sup>, K<sup>+</sup>, and H<sup>+</sup> on an equilibrium between alternative conformations of an RNA pseudoknot. *J. Mol. Biol.* 270: 451–463.

<sup>36</sup>Spedding, G., and Draper, D. E. (1993). Allosteric mechanism for translational repression in the *Escherichia coli* alpha operon. *Proc. Natl. Acad. Sci. USA* 90: 4399–4403.

<sup>37</sup>D'Orval, B. C., *et al.* (1991). RNA secondary structure repression of a muscle-specific exon in HeLa cell extracts. *Science* 252: 1823–1828.